Colloids and Surfaces B: Biointerfaces 200 (2021) 111580

Contents lists available at ScienceDirect

Colloids and Surfaces B: Biointerfaces

journal homepage: www.elsevier.com/locate/colsurfb

Strontium substituted hydroxyapatite with β-lactam integrin agonists to enhance mesenchymal cells adhesion and to promote bone regeneration

Martina Cirillo [a,1], Giulia Martelli [a,1], Elisa Boanini [a,*], Katia Rubini [a], Mara Di Filippo [a], Paola Torricelli [b], Stefania Pagani [b], Milena Fini [b], Adriana Bigi [a], Daria Giacomini [a,*]

[a] Department of Chemistry "G. Ciamician", Alma Mater Studiorum, University of Bologna, Via Selmi 2, 40126, Bologna, Italy
[b] IRCCS Istituto Ortopedico Rizzoli, Complex Structure of Surgical Sciences and Technologies, via di Barbiano 1/10, 40136, Bologna, Italy

ARTICLE INFO

Keywords:
Apatite nanoparticles
β-lactams
Delivery vehicle
Biomedical applications
Osteoinduction
Cell adhesion

ABSTRACT

Multi-functionalization of calcium phosphates to get delivery systems of therapeutic agents is gaining increasing relevance for the development of functional biomaterials aimed to solve problems related to disorders of the muscolo-skeletal system. In this regard, we functionalized Strontium substituted hydroxyapatite (SrHA) with some β-lactam integrin agonists to develop materials with enhanced properties in promoting cell adhesion and activation of intracellular signaling as well as in counteracting abnormal bone resorption. For this purpose, we selected two monocyclic β-lactams on the basis of their activities towards specific integrins on promoting cell adhesion and signalling. The amount of β-lactams loaded on SrHA could be modulated on changing the polarity of the loading solution, from 3.5–24 wt% for compound **1** and from 3.2–8.4 wt% for compound **2**. Studies on the release of the β-lactams from the functionalized SrHA in aqueous medium showed an initial burst followed by a steady-release that ensures a small but constant amount of the compounds over time. The new composites were fully characterized. Co-culture of human primary mesenchymal stem cells (hMSC) and human primary osteoclast (OC) demonstrated that the presence of β-lactams on SrHA favors hMSC adhesion and viability, as well as differentiation towards osteoblastic lineage. Moreover, the β-lactams were found to enhance the inhibitory role of Strontium on osteoclast viability and differentiation.

1. Introduction

The biomedical demand of new materials able to substitute and/or repair damaged biological tissues is growing up continuously. Most biomaterials employed to solve problems related to disorders of the muscolo-skeletal system are based on calcium orthophosphates (CaPs), and in particular on hydroxyapatite (HA), which is the most similar to bone inorganic phase. Recently, the interest toward this class of compounds has stimulated a number of studies aimed at improving their already good biological performances through functionalization with specific additives, including ions, polyelectrolytes and drugs [1,2]. According to the literature [3], the highest number of studies on HA functionalization with inorganic ions has been performed on Strontium. The trend of interest toward this ion has been continuously increasing because of its influence on bone cells. Sr ion is known to counteract abnormal bone resorption by promoting osteoblast proliferation and differentiation and inhibiting osteoclast activity [4,5], being effective also when incorporated into HA [6–11]. Further specific activities towards bone cells can be achieved through multi-functionalization of the calcium phosphate [1,12,13].

To improve tissue/bone regeneration, the efficacy of cell adhesion and differentiation should be enhanced, and in this aspect, integrins could represent an important cellular target [14]. Integrins are transmembrane receptors composed by two protein chains α and β, which upon binding to specific ligands could regulate cell-cell and cell-extracellular matrix interactions. Integrins mediate important cellular events such as adhesion, migration, differentiation, growth, and survival [15,16].

In mammals, 24 different αβ heterodimers have been recognized and some heterodimers are important mediators of bone-cells function [17]. In osteoclasts, for instance, integrin $\alpha_v\beta_3$ is essential for the attachment to matrix proteins of bone and for cell spreading necessary for the bone-resorbing activity [18]. Other integrins might also be involved in osteoclast attachment and function, such as the $\alpha_v\beta_5$ and those with β_1

* Corresponding authors.
E-mail addresses: elisa.boanini@unibo.it (E. Boanini), daria.giacomini@unibo.it (D. Giacomini).
[1] M.C. and G.M. contributed equally

https://doi.org/10.1016/j.colsurfb.2021.111580
Received 1 September 2020; Received in revised form 28 December 2020; Accepted 11 January 2021
Available online 16 January 2021

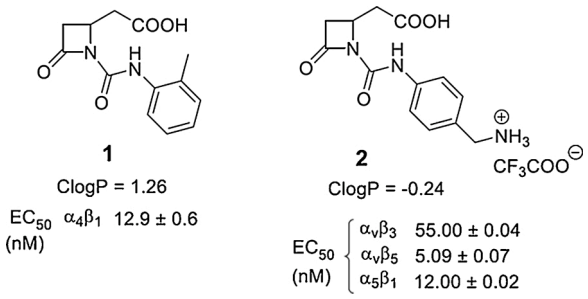

Fig. 1. Compounds **1** and **2** evaluated in this study. The agonist activity of the two β-lactams is reported as EC50 values obtained in cell adhesion test mediated by integrins [34b]. Calculated logP (CLogP) values were obtained with ChemDraw 15.0 program.

and β_2 chains. In addition, also osteoblasts express some integrins able to control their differentiation and fate [19]. One is integrin $\alpha_5\beta_1$, which upon interaction with fibronectin activates pre-osteoblasts to adhere to the extracellular matrix (ECM) and to differentiate into mature osteoblasts [20]. On the contrary, signalling disruption by β_1 integrins results in skeletal defects, and impairment of this signalling in mature osteoblasts decreases osteoblast activity, bone formation and bone mass in growing mice [20,21]. Interestingly, the individual components of $\alpha_5\beta_1$ integrin heterodimer are upregulated in osteoblasts by several anabolic factors, including oestrogens [22], with an implication in the osteoblastogenesis [23].

Biomaterials for bone regeneration should exhibit high cell adhesion to retain effectively anchorage-dependent osteo-progenitors, such as human bone marrow-derived mesenchymal stem cells (MSCs). Moreover, it has been demonstrated that an adequate number of osteoprogenitors is a requisite for an efficient bone repair [24]. MSCs express high levels of several integrin classes [25–27], in particular, integrin α_5 is required for MSC osteogenic differentiation [28], and overexpression of integrin α_4 has been reported to increase the bone-homing of MSCs [29]. Thus, a therapy for bone regeneration could be directed toward integrin receptors on MSCs with a better adhesion to the bone surface [17].

As an alternative to those proteins that are natural ligands of integrins, some cell adhesion peptides containing specific amino acid sequences, such as the RGD tripeptide (Gly–Arg–Asp), were used to functionalize biomaterials for improving tissue integration of artificial implants [30]. In particular, RGD-containing peptides have been shown to augment osteoblasts adhesion to coated surface [31]. The hexapeptide GRGDSP (Gly–Arg–Gly–Asp–Ser–Pro) is another example that demonstrated adhesion activity both in vitro and in vivo in various osteoblastic cells [32]. However, the use of a RGD motif has two main issues: *i)* mimetic peptides may act as partial agonists as well as competitive antagonists of integrins, displaying, in vivo, interactions or competition with endogenous processes [32]; *ii)* the RGD motif can bind to multiple integrin classes, so that the specificity and selectivity of cell activation could be highly limited [33].

Previous studies provided a series of new β-lactam-based molecules able to modulate cell adhesion on targeting different integrins, mainly leukocyte- and RGD-binding integrins such as $\alpha_4\beta_1$, $\alpha_L\beta_2$ $\alpha_v\beta_3$, $\alpha_v\beta_5$, $\alpha_v\beta_6$, $\alpha_5\beta_1$, and $\alpha_{IIb}\beta_3$ [34]. Some of the molecules acted as agonists, promoting cell adhesion and activation of intracellular signalling, others resulted antagonists inhibiting integrin-dependent processes. The structure of the new ligands was designed with the β-lactam ring as a conformational restriction motif that could gain a favourable alignment on the receptor, and molecularly suited for integrin affinity and selectivity.

Functionalization of hydroxyapatite with β-lactam agonists could produce new functional materials with a cell-targeted specificity because of their integrin selectivity. In this paper, we loaded β-lactam integrin agonists onto Strontium substituted hydroxyapatite (SrHA) in order to get innovative materials able to couple the promotion of cell adhesion and activation of intracellular signalling by β-lactam integrin agonists with the beneficial influence of Strontium ion on osteointegration and bone regeneration.

Table 1
Effects of medium on loading of β-lactams **1** and **2** on SrHA.[a].

Entry	Compound (mg)	Solvent (0.6 mL)	Polarity index (PI)[b]	Loading (wt%)[c]
1	1 (10)	CH_3CN	5.8	9.0
2	1 (10)	H_2O/CH_3CN 1:3	6.9	5.3
3	1 (10)	H_2O/ CH_3CN 1:1	8	9.6
4	1 (20)	H_2O/ CH_3CN 1:1	8	24.0
5	1 (6)	H_2O/ CH_3CN 1:1	8	6.2
6	1 (3)	H_2O/ CH_3CN 1:1	8	3.5
7	1 (10)	H_2O/ CH_3CN 3:1	9.1	12.9
8	1 (10)	H_2O/ CH_3CN 10:1	9.8	14.4
9	2 (10)	H_2O/ CH_3CN 1:5	6.5	8.4
10[d]	2 (10)	H_2O/ CH_3CN 1:5	6.5	4.4
11	2 (30)	H_2O/ CH_3CN 1:5	6.5	8.1
12	2 (10)	H_2O/ CH_3CN 1:1	8	4.5
13[e]	2 (5)	H_2O/ CH_3CN 2:1	8.7	3.2
14[e]	2 (10)	H_2O	10.2	4.2

[a] Loading conditions: compound, SrHA (60 mg), solvent (0.6 mL), time (4 h), room temperature.
[b] PI of mixtures was calculated from the Snyder polarity indexes of H_2O and acetonitrile. [ref. 37].
[c] The loaded amount of compounds was evaluated by TGA analysis.
[d] Loading at 70 °C.
[e] Loading overnight.

To this aim, two monocyclic β-lactams **1** and **2** (Fig. 1) were selected on the basis of their activities in cell adhesion tests [34]34b,35]. Compound **1** is a selective agonist of $\alpha_4\beta_1$ integrin with a potency at a nanomolar level and a quite lipophilic character (ClogP = 1.26), whereas **2** has a certain hydrophilicity (ClogP = -0.24) and a wider activity toward integrins $\alpha_v\beta_{3/5}$ and $\alpha_5\beta_1$. Then Sr-HA functionalized with the two agonist ligands were realized for the first time, and fully characterized. In order to demonstrate their potential effectiveness for biomedical applications, biological tests and release of the ligands from the materials were also investigated.

2. Materials and methods

2.1. Synthesis of Sr-hydroxyapatite (SrHA)

SrHA crystals were prepared under nitrogen atmosphere using 50 mL of solution containing $Ca(NO_3)_2{\cdot}4H_2O$ and $Sr(NO_3)_2$ with Sr/(Ca + Sr) molar ratio of 0.1. The total concentration of $[Ca^{2+}] + [Sr^{2+}]$ was 1.08 M. The solution was adjusted to pH 10 with NH_4OH, then heated at 90 °C. Afterwards 50 mL of 0.65 M $(NH_4)_2HPO_4$ was added dropwise under stirring. The resulting slurry was kept at 90 °C for 5 h, then the precipitate was isolated by centrifugation (10,000 rpm, 10 min), washed twice with distilled water, and air-dried at 37 °C.

2.2. Synthesis of β-lactams 1 and 2

Compounds **1** and **2** were synthesized according to an optimized multi-step procedure (Fig. S1) [34b]. Structures of the compounds were assessed by ^1H NMR, purities resulted to be ≥ 95 % by HPLC-UV analyses.

The stabilities of compounds **1** and **2** in buffered water solutions at pH = 7.4 and in physiological solution at 30 °C were studied by HPLC-UV analysis at 254 nm (please see Supporting Information Fig. S2).

2.3. β-Lactams loading on SrHA

β-Lactams **1** and **2** were loaded on SrHA as follows: the β-lactam (10 mg) was diluted in a 10 mL flask in the appropriate H_2O/MeCN mixture

(0.6 mL) (see Table 1), then SrHA nanoparticles (60 mg) were added at room temperature (or 70 °C, Table 1). After selected time (Table 1) the mixture was centrifuged for 5 min. at 1200 rpm. Then, the solid phase was dried at 48 °C for 48 h, and maintained in desiccator ($CaCl_2$) for 24 h before the analyses. Determination of the quantity of the β-lactams loaded on SrHA was assessed by thermogravimetric analysis (TGA) on the dried samples and data were reported in Table 1.

The samples are indicated as SrHA**Y**-X, where **Y** indicate the two different β-lactam compounds (**1** and **2**) and X their amount expressed as wt%.

2.4. Release studies

The in vitro release profiles of β-lactams **1** and **2** from the corresponding SrHA samples were evaluated at 37 °C in triplicate by HPLC-UV analysis, using linear calibration curves obtained at 254 nm. Data were reported as mean values ± standard deviations. Release studies were performed on samples with a compound loading of 12.9 and 6.2 wt % for SrHA**1**, and of 8.4 and 4.2 wt% for SrHA**2**. Measurement were performed at selected times on the supernatant, which was separated and substituted with fresh solution (refresh). Results were expressed as cumulative release in mol% (of the total loaded amount) over the refresh number and over the time (Supplementary Information).

2.5. Characterization methods

The samples SrHA**1**-12.9 and SrHA**2**-8.4 were analysed to get ATR-FTIR spectra with Alpha FT IR Bruker spectrometer with ATR diamond module at single reflection, with a resolution of 4 cm^{-1} and 32 scans in the scan range 4000–450 cm^{-1}. The background spectrum was collected before the acquisition of each sample spectrum. HPLC-MS analyses were obtained with an HP1100 instrument Agilent Technologies (ZOBRAX-Eclipse XDB-C8 column, H_2O/CH_3CN, 0.4 mL/min, from 30 to 80 % of CH_3CN in 8 min, 80 % of CH_3CN until 25 min) integrated with a MSD1100single-quadrupole mass spectrometer (full scan mode, *m/z* 50–2600, scan time 0.1 s, positive ion mode, ESI spray voltage 4500 V, N_2 35 psi, drying gas flow 11.5 mL/min, fragmentor voltage 20 V. ^1H NMR spectra were recorded with an INOVA 400 instrument with a 5 mm probe, as $CDCl_3$ or d-4 methanol solutions.

Powder X-ray diffraction patterns were recorded from 10 to 60 2θ° with a step size of 0.1° and time/step of 100 s (PANalytical-X'Pert PRO powder diffractometer equipped with a fast X'Celerator detector,λ = 0.154 nm, 40 mA, 40 kV).

For Transmission Electron Microscopy (Philips CM-100) investigations, a small amount of powder was dispersed in ethanol and submitted to ultrasonication.

Ca and Sr contents in the solid products were monitored by ion cromatography (Dionex ICS-90). Powders were previously dissolved in 0.1 M HCl.

Thermogravimetric analysis was carried out heating under air stream from 40.0 °C at 10.0 °C/min in a TGA7 Perkin Elmer instrument.

2.6. In vitro tests

Biological tests were performed on samples of SrHA functionalized with β-lactam compounds **1** or **2** (Y) in different percentage (X). Samples were prepared by pressing 40 mg of SrHA**Y**-X powder into cylindrical molds using a standard evacuable pellet die (Hellma). The obtained disk-shaped samples (diameter =6 mm, height = 1.5 mm) were sterilized by gamma irradiation (25 kGy).

2.6.1. In vitro co-culture model

The in vitro model was performed culturing together primary osteoclast derived from mononucleated blood cells (OC), and primary mesenchymal stem cells derived from bone marrow (hMSC, ATCC), both from human origin.

Osteoclast precursors were isolated from mononuclear cells of peripheral blood of healthy donor (Ethic Committee approval n.191/2019/Sper/IOR, prot. VIRTOS). Briefly, a volume of peripheral blood, diluted 1:1 with pre-warmed PBS, was carefully layered on an equal volume of Histopaque1077, to separate the mononuclear cells from the other elements of blood by density gradient centrifugation (600 *g*, room temperature, 30 min). The mononuclear cells at the interface PBS/Histopaque were collected after centrifugation, washed twice in PBS, and seeded on the bottom of 24-wells plates (4×10^5 cells/well) using the culture medium (DMEM, Sigma, UK) supplemented with osteoclastogenic factors (macrophage colony-stimulating factor, MCSF, 25 ng/mL, and receptor activator for κB factor ligand, RANKL, 30 ng/mL, DMEM-OC). The plate was maintained for 7 days in standard condition (37 °C ± 0.5 temperature, 5% CO_2 ± 0.2, 95 % humidity), to differentiate in osteoclasts (OC).

A culture of hMSC was expanded in their basal medium. After counting, cells were seeded on material samples (4×10^4 cells/sample) prepared with different concentrations of β-lactams (SrHA**1**-3.5, SrHA**1**-6.2, SrHA**2**-3.2, SrHA**2**-4.2), and on SrHA without lactams as reference group. Samples with cells were co-cultured in the same wells with OC, as showed in Fig. S3, for 14 days. Final medium was a mixture of osteogenic differentiation medium (StemPro Gibco, Termofisher, USA) and DMEM-OC.

Additional control groups with only cells (CTR-hMSC and CTR-OC cultures) were prepared to verify regular cell proliferation and differentiation, regardless of material presence.

2.6.2. Cell viability and adhesion

Cell viability was tested by Alamar blue dye (Cell Viability Reagent, LIFE Technologies Corp., Oregon, USA). Samples with hMSC were transferred in new empty wells to evaluate hMSC separately from OC, both at 7 and at 14 days of co-culture. The reagent, which was added 1:10 reagent/medium to each well and incubated for further 4 h at 37 °C, contains a redox indicator that modify the color from blue to pink according to the increasing number of living cells.

Cell colonization of samples was observed after DAPI staining (Sigma Aldrich, Steinheim, Germany), performed on hMSC adherent to material samples, according to manufacturer's instructions. Briefly, after passages in PBS, 4% paraformaldehyde, 0.5 % Triton X-100, and DAPI solution, nuclei of cells on samples were observed in fluorescence by inverted microscope (Eclipse TiU, NIKON Europe BV, NITAL SpA, Milan, Italy) equipped with a digital camera.

2.6.3. Cell differentiation and morphology

The evaluation of osteoclast differentiation was performed using TRAP (Tartrate-resistant acid phosphatase) staining (TRAP kit, SIGMA, Buchs, Switzerland), following manufacturer's instructions, on control culture after 4 weeks of culture, and on cells cultured with hMSC, alone or in presence of materials, after 10 days of co-culture.

TRAP staining develops red colour in positive cells, allowing to evaluate osteoclastogenesis. The number of TRAP positive cells, typically showing 3 or more nuclei each positive cell, were counted in 10 fields under the microscope by a semiautomatic software (NIS-Elements AR 4.30.01). Results are given as percentage, considering OC control culture as 100 %.

Moreover, osteoclast morphology was evaluated by Phalloidin / DAPI staining according to manufacturer's instructions, and observed by a computerized image analysis system (Kontron KS 300 software, Kontron Electronic GmbH, Eching bei Munchen, Germany).

FITC-conjugate phalloidin solution shows cytoskeleton and it is useful to visualize cell shape and adhesion onto material surface.

Random samples of materials cultured with hMSC were treated for scanning electron microscopy (SEM) at the end of experimental time and examined with a Hitachi S-2400 instrument operating at 15 kV.

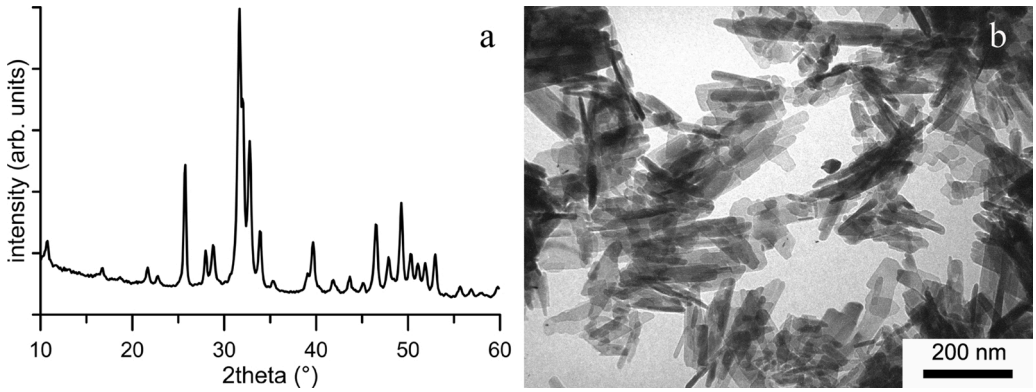

Fig. 2. X-ray diffraction pattern (a) and TEM image (b) of SrHA nanocrystals.

2.6.4. qPCR

qPCR technique was used to evaluate most common markers of co-cultured hMSC and OC to assess gene expression of cell differentiation and activity. Total RNA was extracted from samples cultured with materials and controls (only cells) both at 7 and 14 days by PureLink RNA Mini Kit (Life Technologies, Carlsbad, CA, USA) and samples were reverse transcribed with SuperScriptVILO cDNA Synthesis Kit (Life Technologies, Carlsbad, CA, USA), following the manufacturer instructions. Semi-quantitative polymerase chain reaction (PCR) analysis was performed for each sample in duplicate in a LightCycler 2.0 Instrument (Roche Diagnostics GmbH, Manheim, Germany) using QuantiTect SYBR Green PCR Kit (Qiagen, Hilden, Germany) and gene-specific primers (Table S1). After melting curve analysis to check for amplicon specificity, the threshold cycle was determined for each sample and relative gene expression was calculated using the $2^{-\Delta\Delta}$CT tmethod. For each gene, expression levels were normalized to GAPDH (Glyceraldehyde 3-phosphate dehydrogenase, Invitrogen, CA, USA) using SrHA reference group for each experimental time as calibrator.

Statistical analysis: Statistical evaluation of data was performed using the software package SPSS/PC + Statistics TM 23.0 (SPSS Inc., Chicago, IL USA). The results presented are the mean of six independent values. Data are reported as mean ± standard deviations (SD) at a significance level of $p < 0.05$. After having verified normal or not distribution and homogeneity of variance, a post-hoc test was applied.

3. Results and discussion

Among the series of integrin ligands previously synthesized [34], **1** and **2** were selected for this study on the basis of their integrin specificity, agonism, and lipophilicity/hydrophilicity character. According to this aspect, the *N*-substituent on the lactam ring confers a specific behaviour: compound **1** with the *o*-tolylurea is quite lipophilic as indicated by its ClogP, whereas **2** with a *p*-aminobenzyl moiety is more hydrophilic (Fig. 1).

As mentioned above, Strontium substituted hydroxyapatite (SrHA) was chosen because the beneficial influence of Sr ion on osteointegration and bone regeneration. The synthesized SrHA was characterized by the powder X-ray diffraction pattern (Fig. 2) that showed the characteristic peaks of hydroxyapatite shifted towards smaller angles, in agreement with greater lattice parameters. Indeed, the values of the calculated lattice parameters (a = 9.453 (3) Å, c = 6.903(4) Å) indicated an enlargement of the unit cell in comparison to that characteristic of pure HA (PDF: 9–432) coherently with a partial substitution of Sr ion to Ca ion into the hydroxyapatite structure. Moreover, SrHA nanocrystals, which contain about 7.5 ± 0.2 at% of Strontium (calculated with respect to total cations), displayed a plate-like shape with mean dimensions of about 150 nm x 30 nm.

3.1. Loading conditions

The loading of β-lactams **1** and **2** on SrHA nanocrystals was screened in H_2O or H_2O/acetonitrile mixtures to evaluate the medium effect on the loading. Acetonitrile was chosen as co-solvent upon the good results obtained in a previous study with antibacterial *N*-methylthio-β-lactams loaded on hydroxyapatite nanocrystals [36]. The influence of the compound concentration and on the polar character of the loading solution [37] was also explored (Table 1).

The amount (wt%) of β-lactams loaded on SrHA was evaluated through TGA analysis on dried samples. Examples of TGA plots are reported in Fig. S4. When the loading was carried out in acetonitrile, a good uptake from the solution was observed (9 wt%, Table 1 entry 1), the loading in water alone, instead, was hindered by the insolubility of **1**. The polarity of the medium polarity was varied through variation of the composition of the H_2O/acetonitrile mixtures at constant concentration (0.063 M). Data in Table 1 showed that the loading amount of compound **1** increased as the polarity raised (Table 1 entries 2, 3, 7 and 8), from 5.3 wt% in H_2O/CH_3CN = 1:3 (PI = 6.9) to 14.4 wt% in H_2O/CH_3CN = 10:1 (PI = 9.8). This could be rationalized considering that the molecule **1** is quite apolar (ClogP = 1.26) with high affinity to acetonitrile, so that the adsorption of compound **1** on SrHA was more favoured from a water enriched solution. Compound **1** is hydrophobic and its solvation in acetonitrile is destabilized by an increase of water amount in the loading solution, which promotes its adsorption on SrHA [38]. Moreover, in H_2O/CH_3CN 1:1 mixture the loaded wt% of **1** is proportional to the β-lactam concentration, resulting higher on increasing the amount of the compound in the starting solution (Table 1 entries 3–6). In particular, charging 20 mg of **1** per 0.6 mL of the 1:1 solvent mixture gave the highest loading amount, 24 wt% (Table 1 entry 4).

Conversely, SrHA**2** composites settled around a medium-low loading (3.2–8.4 %) that decreased on increasing the solvent polarity (Table 1 entries 9, 12, and 13). To notice, the lowest value of loaded β-lactam (3.2 wt% Table 1 entry 13) arose from a half content of β-lactam **2** in an enriched water solution, balanced by a prolonged loading time (overnight). Compound **2** is more polar and hydrophilic (CLogP = -0.24) than **1**, and hence it tends to be better distributed in solutions at higher water content than to be adsorbed on SrHA. Neither tripling concentration (Table 1, entry 11), nor increasing of the loading temperature (70 °C, Table 1, entry 10) enhanced loading. The absorption in H_2O alone gave a loading of 4.2 % (Table 1, entry 14), even if conducted overnight, whereas the experiment in acetonitrile alone was not feasible due to the insolubility of **2** in this solvent.

As a general comment on the loading, the two β-lactam compounds **1** and **2** were adsorbed on SrHA as a function of their partition between the solid phase and the loading solution: SrHA in fact competes with the solvent for the recruitment of β-lactam compounds, which in turn depends on the polarity of the compound and of the loading solution.

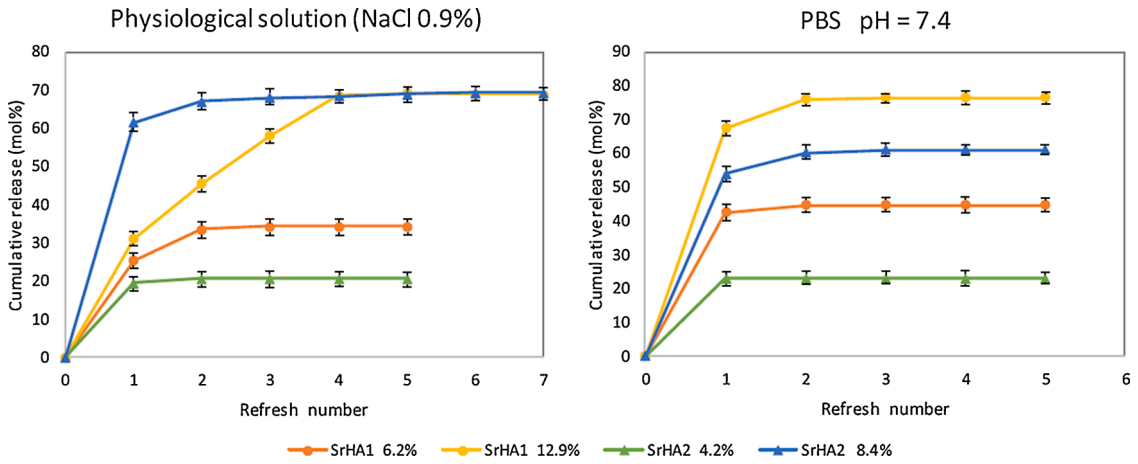

Fig. 3. Release of β-lactams compound **1** (●) from SrHA1 and compound **2** (▲) from SrHA2 samples. The different wt% loading of the composites are in the legend. The cumulative release is reported as mol % respect to the loaded amount.

3.2. Characterization of SrHA composites with the β-lactams

The new β-lactam-functionalized SrHA composites were characterized by ATR-FTIR spectroscopy that shed light on the interactions between β-lactams **1**-**2** and hydroxyapatite. Infrared spectra of SrHA**1**-12.9 in comparison with compound **1** alone, and SrHA**2**-8.4 in comparison with compound **2** alone are reported in Fig. S5. IR spectra of SrHA composites display the O—H stretching and bending modes of hydroxyapatite at 3572 and 630 cm^{-1} respectively, the strong bands due to phosphate absorption at 550–630 and 900−1100 cm^{-1}, together with the bands of the β-lactam compounds (full spectra in Supplementary Information, Fig. S6 and S7). Fig. S5 reports a selected range of ATR-FTIR spectra (2000−400 cm^{-1}) for a better comparison between the SrHA composites and the compounds alone. Compound **1** showed three C═O stretching bands at 1761 (β-lactam), 1715 (COOH), and 1695 cm^{-1} (urea). In the composite SrHA**1** the band corresponding to the C═O stretching of the COOH was no longer observed, as well as the band at 1309 cm^{-1} relative to the CO stretching of the carboxylic acid dimer. Conversely, two new intense bands appeared in the composite: one at 1570 cm^{-1} (near the ureidic amide band II at 1551 cm^{-1}), and another at 1440 cm^{-1} that could be both attributed to the asymmetric and symmetric stretching of a carboxylate anion, respectively. This analysis supported the hypothesis that β-lactam **1** could have been absorbed onto the SrHA as a carboxylate anion through ionic interactions with Sr^{2+} or Ca^{2+}. Moreover, since we detected a gap between the two bands of the carboxylate anion minor than 200 cm^{-1}, in our case $\Delta\nu = 130$, it could be formulated a hypothesis of a monodentate coordination of the carboxylate on the apatite [39]. In compound **2** the three C═O bands were observed at 1773 (β-lactam), 1703 (COOH), and 1658 cm^{-1} (urea), respectively, whereas in the composite SrHA**2** only the C═O of the urea slightly moves to 1680 cm^{-1}. This could account for a less tendency of **2** to form a carboxylate anion upon the adsorption on SrHA if compared to compound **1**, maybe because **2** could establish interactions between the ammonium cation residue and the negatively charged phosphate groups on SrHA surface. The consistency of the β-lactam C═O stretching in pure compounds with those in Sr-HA composites provides strong evidence of the integrity of β-lactam compounds upon adsorption on Sr-HA.

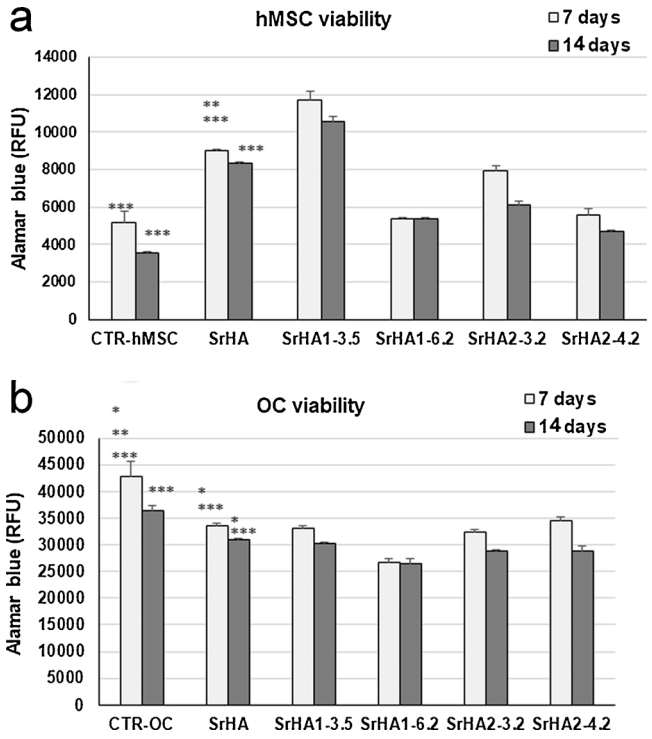

Fig. 4. Viability of hMSC (a) and OC (b) after 7 (light bars) and 14 (dark bars) days of co-culture with biomaterials and controls (cells only) by Alamar blue test. Statistical analysis (T2 Tamhane post-hoc test) is reported in the figure (*$p < 0.05$, **$p < 0.005$, ***$p < 0.0005$).
hMSC - 7 days: ***CTR-hMSC vs SrHA**1**-3.5, SrHA**2**-3.2, SrHA; ***SrHA vs SrHA**1**-3.5) SrHA1-6.2, SrHA**2**-4.2; **SrHA vs SrHA**2**-3.2; 14 days: ***CTR-hMSC vs SrHA**1**-3.5, SrHA**1**-6.2, SrHA**2**-3.2, SrHA**2**-4.2, SrHA; ***SrHA vs SrHA**1**-3.5, SrHA**1**-6.2, SrHA**2**-3.2), SrHA**2**-4.2.
OC - 7 days: *CTR-OC vs SrHA**1**-3.5, SrHA**2**-4.2, SrHA; **CTR-OC vs SrHA**2**-3.2; ***CTR-OC, SrHA vs SrHA1-6.2; *SrHA vs SrHA**2**-3.2; 14 days: ***CTR-OC vs SrHA**1**-3.5, SrHA**1**-6.2, SrHA**2**-3.2, SrHA**2**-4.2, SrHA; ***SrHA vs SrHA**1**-6.2, SrHA**2**-3.2; *SrHA vs SrHA**2**-4.2.

3.3. Release studies from SrHA1 and SrHA2 composites

The in vitro release of β-lactams **1** and **2** from the SrHA composites at different wt% loading was determined through HPLC-UV analysis on supernatant solutions after each refresh (Fig. 3). Two aqueous solutions were analysed: a saline solution and a phosphate buffered solution at pH = 7.4 as models for physiological conditions. At first, it was observed that a new release occurred just after refreshing the aqueous solution, thus the release was determined as cumulative amount over the refresh number.

The release of both compounds in the aqueous media showed an initial burst followed by a steady concentration-dependent profile. Higher concentrations in the SrHA-β-lactam composite released higher amounts of compounds, except for SrHA**1**-12.9 that has a cumulative release similar to SrHA**2**-8.4 in physiological solution. A further

peculiarity of SrHA**1**-12.9 in saline solution regards its more gradual release over time than the other composites; a steady concentration-dependent profile is indeed gained at the fourth refresh, compared to the second in the other SrHA-β-lactams. Generally, for compound **1** the saline solution allowed slightly slower release from SrHA**1** compared to the phosphate buffer. For compound **2** instead, the release rates are comparable in both aqueous solutions. Noteworthy, compounds **1** and **2** were not completely released from the composites, thus significant amounts of the β-lactams remained adsorbed on SrHA allowing a persistent bioactivity over time. Only SrHA**1**-3.5 %, the lowest loaded concentration of compound **1**, released all the adsorbed compounds (release over time in Supplementary Material, Figs. S8 and S9).

Structural, morphological and chemical investigations of the samples after β-lactams release indicate no significant modifications. After release, the crystals appear just a bit fractured in comparison with pristine powders, as shown in the TEM images of two typical samples reported in Fig. S10. In agreement, the diffraction peaks present in the X-ray patterns of the same samples (Fig. S10) appear just slightly broader than those reported in Fig. 2. Furthermore, the results of chemical analysis showed no significant variation of Strontium content.

3.4. *In vitro tests*

Some selected samples of SrHA functionalized with different contents of β-lactam integrin agonists were submitted to in vitro cell tests. Low content samples in β-lactams were selected to avoid interfering toxicity effects, and a co-culture model of human primary mesenchymal stem cells (hMSC) and human primary osteoclasts (OC) were chosen in order to investigate the influence of the functionalized materials on hMSC adhesion, viability and differentiation, as well as on OC viability and activity.

3.4.1. *Osteoblast and osteoclast viability*

hMSC proliferated regularly in control wells as well as in those with the functionalized materials. Considering CTR-hMSC as 100 % of viability, samples reached higher values of viability when co-cultured on SrHA, SrHA**1**-3.5 and SrHA**2**-3.2 at both 7 and 14 days, and on SrHA**1**-6.2 and SrHA**2**-4.2 at 14 days (Fig. 4a). Moreover, hMSC viability was significantly higher on SrHA**1**-3.5 than on SrHA (7 and 14 days). The data showed that in comparison with CTR-hMSC, cells grown onto the new biomaterials demonstrated a significant enhancement of proliferation. In particular, it was observed a greater hMSC viability on those functionalized SrHA materials with a lower content of β-lactams.

Moreover, cell adhesion was evaluated by DAPI: onto all biomaterials, cells nuclei (DAPI staining) appeared well defined and covered the surface, suggesting that cells colonized all samples (Fig. S11). Results were in line with viability data obtained by Alamar Blue test and demonstrated that all samples promote cell adhesion and proliferation. In agreement, SEM images show that cells are rich of filopodia and well attached and spread on samples SrHA**1**-3.5 and SrHA**2**-3.2 (Fig. S12).

All these observations agree to what is known about integrins: these transmembrane proteins, by binding extracellular matrix residues, are able to trigger a number of cellular events aimed to enhance cell proliferation, migration and differentiation [40]. The link between cell and matrix represents an important signal for the growth of anchorage-dependent cells, allowing cell survival with respect to apoptosis [41]. An interesting study by Di Benedetto et al. described expression and localization of single integrin subunits αv and β3 in mesenchymal cells differentiating toward osteoblasts: both subunits progressively increased upon the time and reorganized their distribution on cellular membrane [42].

Furthermore, α4β1, αvβ3, αvβ5 bind osteopontin (OPN), so eliciting the already cited functions of adhesion, survival, and migration [43]. The observed response of hMSCs in term of viability, proliferation and adhesion indicates a correct stimulation of the aforementioned integrins

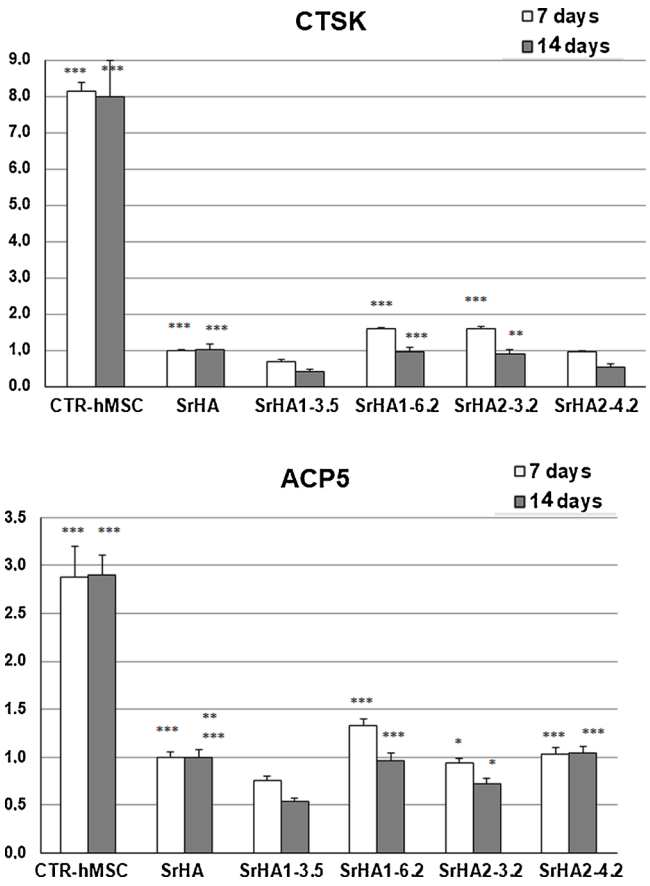

Fig. 5. Gene expression of common markers CTSK and ACP5 of osteoclast differentiation by qPCR, after 7 (light bars) and 14 (dark bars) days. Results were normalized to GAPDH expression and data are given as fold change relative to the reference group (SrHA), considered as 1. Results are the mean (+/- sd) of six replicates. Statistical analysis (Scheffè post hoc test) is reported in the figure (*$p < 0.05$, **$p < 0.005$, ***$p < 0.0005$).
CTSK - 7 days: ***CTR-OC vs all; ***SrHA vs SrHA1-3.5, SrHA1-6.2, SrHA2-3.2; ***SrHA1-6.2, SrHA2-3.2 vs SrHA1-3.5, SrHA2-4.2; 14 days: ***CTR-OC vs all; ***SrHA vs SrHA1-3.5, SrHA2-4.2) ***SrHA1-6.2 vs SrHA1-3.5, SrHA2-4.2; ** SrHA2-3.2 vs SrHA1-3.5, SrHA2-4.2.
ACP5 - 7 days: ***CTR-OC vs all; ***SrHA vs SrHA1-3.5, SrHA1-6.2; ***SrHA1-6.2 vs SrHA1-3.5, SrHA2-3.2, SrHA2-4.2; * SrHA2-3.2 vs SrHA1-3.5; *** SrHA2-4.2 vs SrHA1-3.5; 14 days: ***CTR-OC vs all; **SrHA vs SrHA2-3.2; ***SrHA vs SrHA1-3.5; *** SrHA1-6.2, SrHA2-4.2 vs SrHA1-3.5, SrHA2-3.2; * SrHA2-3.2 vs SrHA1-3.5, SrHA1-3.5.

carried out by these β-lactams, which represent their agonists. This strategy, similar to the functionalization of biomaterial surfaces with ECM proteins, could improve the bone reconstruction, also by inducing the expression of membrane receptors on the involved cells [42].

All samples, as expected, exhibited lower viability of OC than CTR-OC, both at 7 and at 14 days of culture (Fig. 4b). The values recorded for SrHA**1**-6.2, SrHA**2**-3.2 (7 and 14 days), and SrHA**2**-4.2 (14 days) were also lower than that of SrHA. These data not only confirm the inhibiting effect of Sr on osteoclasts viability [7,8], but also indicate that this effect is enhanced by the presence of the functionalizing molecules.

3.4.2. *Osteoclast differentiation*

Osteoclast of CTR group (CTR-OC) were stained with Phalloidin / DAPI after 3 weeks of culture. Images in Fig. S13a show the formation of large multinucleated cells (fluorescent green, nuclei blue). After further 7 days, TRAP staining (Fig. S13b) confirmed that the isolated mononucleated cells have fused forming polynucleated purple TRAP positive cells, characteristics of differentiated osteoclasts. At the end of experimental time, also co-cultured cells of different groups, with or without

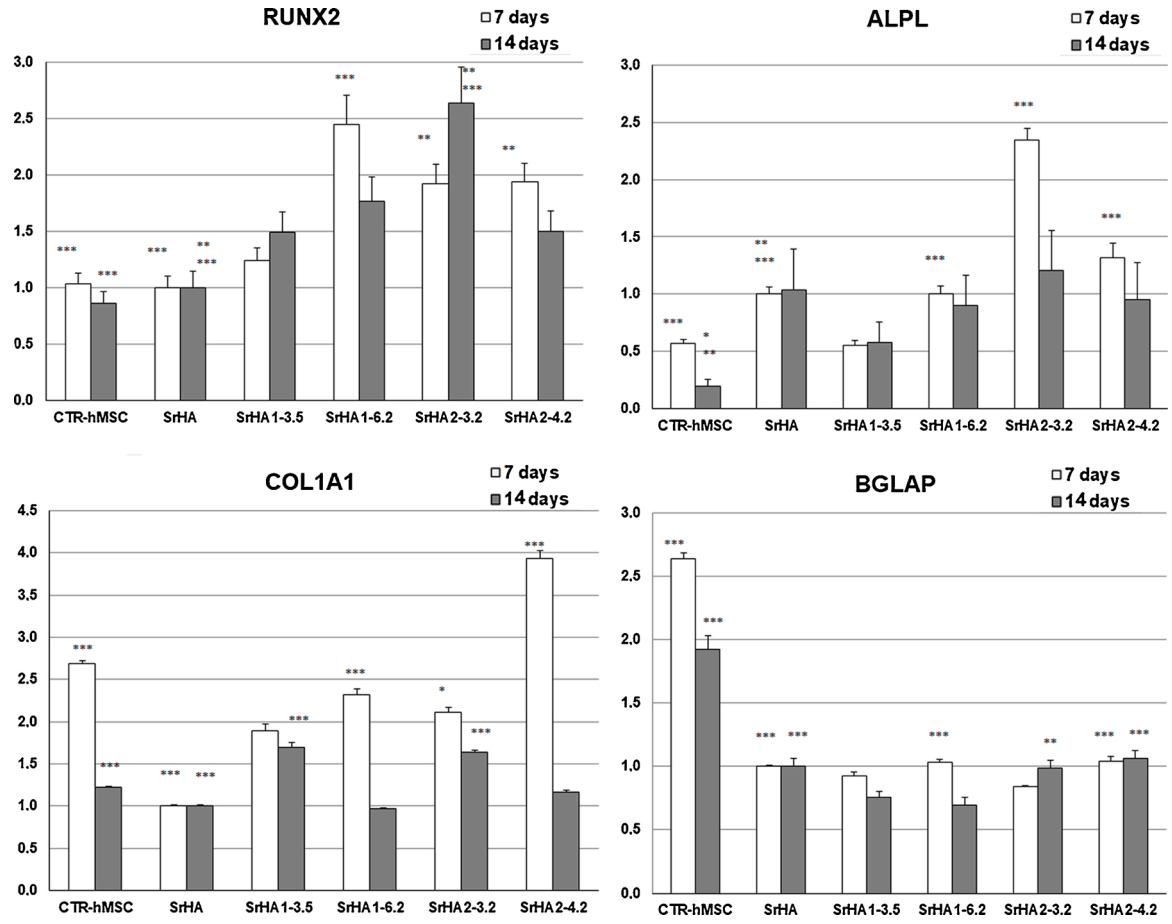

Fig. 6. Gene expression of common markers of osteoblast differentiation RUNX2, ALPL, COL1A1, and BGLAP by qPCR, after 7 (light bars) and 14 (dark bars) days. Results were normalized to GAPDH expression and data are given as fold change relative to the reference group (SrHA), considered as 1. Results are the mean (+/- sd) of six replicates. Statistical analysis is reported in the figure (*$p < 0.05$, **$p < 0.005$, ***$p < 0.0005$).

RUNX2 - 7 days: ***CTR-hMSC, SrHA vs SrHA**1**-6.2, SrHA**2**-3.2, SrHA**2**-4.2; *** SrHA**1**-6.2 vs. SrHA**1**-3.5; ** SrHA**2**-3.2, SrHA**2**-4.2 vs SrHA**1**-3.5; 14 days: ***CTR-hMSC vs. SrHA**1**-6.2, SrHA**2**-3.2; **SrHA vs SrHA**1**-6.2; ***SrHA vs SrHA**2**-3.2; *** SrHA**2**-3.2 vs SrHA**1**-3.5, SrHA**2**-4.2; ** SrHA**2**-3.2 vs SrHA**1**-6.2).

ALPL - 7 days: ***CTR-hMSC vs SrHA**1**-6.2, SrHA**2**-3.2, SrHA**2**-4.2; **SrHA vs SrHA**2**-4.2; ***SrHA vs CTR-hMSC, SrHA**1**-3.5, SrHA**2**-3.2; *** SrHA**1**-6.2 vs SrHA**1**-3.5; *** SrHA**2**-3.2 vs SrHA**1**-3.5, SrHA**1**-6.2, SrHA**2**-4.2; *** SrHA**2**-4.2 vs SrHA**1**-3.5, SrHA**1**-6.2; 14 days: *hMSC vs SrHA, SrHA**1**-6.2, SrHA**2**-4.2; **hMSC vs SrHA**2**-3.2.

COL1A1 - 7 days: ***CTR-hMSC vs all; ***SrHA vs SrHA**1**-3.5, SrHA**1**-6.2, SrHA**2**-3.2, SrHA**2**-4.2; ***SrHA**1**-6.2) vs SrHA**1**-3.5; * SrHA**2**-3.2 vs SrHA**1**-3.5, SrHA**1**-6.2; *** SrHA**2**-4.2 vs SrHA**1**-3.5, SrHA**1**-6.2, SrHA**2**-3.2; 14 days: ***CTR-hMSC vs SrHA, SrHA**1**-3.5, SrHA**1**-6.2, SrHA**2**-3.2; ***SrHA vs SrHA**1**-3.5, SrHA**2**-3.2, SrHA**2**-4.2; *** SrHA**1**-3.5, SrHA**2**-3.2 vs SrHA**1**-6.2, SrHA**2**-4.2.

BGLAP - 7 days: ***CTR-hMSC vs all; ***SrHA, SrHA**1**-6.2, SrHA**2**-4.2 vs SrHA**2**-3.2; 14 days: ***CTR-hMSC vs all; ***SrHA, SrHA**2**-4.2 vs SrHA**1**-3.5, SrHA**1**-6.2; ** SrHA**2**-3.2 vs SrHA**1**-3.5, SrHA**1**-6.2.

biomaterials, were stained with TRAP. Results are shown in Fig. S13c. When compared to CTR-OC group, considered as 100 %, all other groups (reference SrHA and different β-lactam-composite groups) showed significantly lower percentage ($p < 0.0005$) of TRAP positive cells, as a direct effect of Sr presence in the samples.

3.4.3. qPCR

The most common genes for osteoclast and osteoblast differentiation and activity were analyzed to assess the effects of biomaterials on co-cultured cells behavior. All results were normalized to GAPDH expression and data are given as fold change relative to the reference group (SrHA), considered as 1.

The effect on osteoclast differentiation of mononucleated cells was studied comparing Cathepsin K (CTSK) and Acid phosphatase 5 (ACP5) gene expression in CTR-OC, SrHA and β-lactam-SrHA groups. CTSK is highly expressed in osteoclast and contribute to bone resorption with degradation of type I collagen [44]. ACP5 that encodes for TRAP, under the stimulation of RANKL affects different pathways related to bone resorption and osteoclast activity [45]. Both CTSK and ACP5 were highly expressed in CTR-OC, whereas they were significantly reduced in SrHA already at 7 days, with no changes at 14 days, confirming the inhibiting effect of Strontium on osteoclast differentiation (Fig. 5). The effects of Sr on the osteoclasts' activity have been known from several years: anti-osteoporotic drugs, such as strontium ranelate, are used to improve the clinical conditions in osteoporosis, accelerate the bone fracture healing, and improve the implant fixation and osseointegration [46,47].

The level of activation of the two genes were also significantly lower on β-lactam functionalized samples than on CTR-OC; moreover, the values of CTSK in SrHA**1**-3.5 and SrHA**2**-4.2, and of ACP5 in SrHA**1**-3.5 and SrHA**2**-3.2, were even significantly lower than on SrHA.

Osteoblastic differentiation of hMSC was investigated through evaluation of the gene expression of Runt-related transcription factor 2 (RUNX2). RUNX2 is a transcriptional factor that induces mesenchymal stem cell toward osteoblast lineage and its expression is upregulated in immature osteoblasts [48]. The evaluation of RUNX2 in SrHA and CTR-hMSC groups showed that Sr did not influence hMSC differentiation toward osteoblastic lineage. Indeed, no differences in RUNX2 gene

expression were found between SrHA and CTR-hMSC, both at 7 (1.00+/-0.10 and 1.035+/-0.09 respectively) and at 14 (1.005+/-0.15 and 0.86+/-0.10 respectively) days. On the contrary, the comparison between the results obtained on β-lactam functionalized samples and on SrHA demonstrated that all the different formulations positively influenced RUNX2 expression, even if with different statistical significance (Fig. 6).

Osteoblastic activity was also investigated through analysis of further representative genes, such as ALPL, COLL1A1, and BGLAP, which encodes for alkaline phosphatase (ALP), type I collagen (COLL1) and osteocalcin (OSTC), respectively. ALP is an early marker of differentiation, COLL1 is the major constituent of the extracellular bone matrix and OSTC is one of the most abundant non-collagen proteins produced by differentiated osteoblasts.

The results indicate that all the samples promote ALPL expression. In particular, ALPL expression on SrHA was significantly greater than on CTR-hMSC. Moreover, all the functionalized samples, with the only exception of SrHA**1**-3.5, displayed significantly higher ALPL than SrHA at 7 days, whereas at 14 days the values for all the functionalized groups were not statistically different from SrHA.

COL1A1 expression showed lower levels on SrHA group than on CTR-hMSC both at 7 and 14 days. However, results of all β-lactam functionalized groups were significantly higher in comparison with SrHA at 7 days, and the value measured on SrHA**2**-4.2 was also significantly higher than on CTR-hMSC. At 14 days COL1A1 expression on all functionalized materials was greater or not significantly different than on SrHA, with SrHA**1**-3.5 and SrHA**2**-3.2, exhibiting even higher values than CTR-hMSC.

BGLAP also was lower on SrHA when compared to CTR-hMSC (7 and 14 days). The results obtained on functionalized materials were similar to those on SrHA, with the exception of a lower BGLAP expression on SrHA**2**-3.2 at 7 days and on SrHA**1**-3.5 and SrHA**1**-6.2 at 14 days (Fig. 6).

It can be concluded that the presence of β−lactams on functionalized samples positively influenced gene expression, which generally reached levels of activation higher than or equal to the reference SrHA group.

4. Conclusions

Multifunctionalized materials were obtained by loading β-lactam integrin agonists on Strontium substituted hydroxyapatite. The amount of β-lactam compounds onto Sr-hydroxyapatite could be modulated through variation in the polarity of the loading solution. After an initial burst, the release of both β-lactams in aqueous solution reached a steady state, maintaining a significant local concentration over time.

The results of in vitro tests showed that functionalized samples promoted adhesion and enhanced the viability of human mesenchymal stem cells. Regarding the effect of β-lactams on mesenchymal stem cells differentiation into osteoblastic lineage, results showed that after 14 days of co-culture, mesenchymal stem cells were directed to osteoblast differentiation, as stated by Runt-related transcription factor 2 (RUNX2) activation, which reached higher levels than control and reference groups. The higher expression of alkaline phosphatase ALPL and collagen type I alpha 1 chain (COL1A1), and the lower levels of bone gamma-carboxyglutamate protein (BGLAP) in comparison to control and/or reference group suggested that cells after 14 days were in the first phases of differentiation. Moreover, the presence of β-lactam integrin agonists enhanced the inhibiting influence of Sr-hydroxyapatite on osteoclast viability and activity, but at the same time the Sr ion contributed to supporting osteogenic differentiation of hMSCs [49], suggesting that these multi-functionalized materials can be employed locally to promote osteointegration and counteract abnormal bone loss.

Declaration of Competing Interest

The authors declare that they have no known competing financial interests or personal relationships that could have appeared to influence the work reported in this paper.

CRediT authorship contribution statement

Martina Cirillo: Investigation, Data curation, Validation. **Giulia Martelli:** Investigation, Data curation, Validation. **Elisa Boanini:** Conceptualization, Methodology, Supervision, Resources, Visualization, Writing - original draft, Writing - review & editing. **Katia Rubini:** Investigation, Data curation, Validation. **Mara Di Filippo:** Investigation. **Paola Torricelli:** Investigation, Data curation, Validation, Writing - original draft. **Stefania Pagani:** Investigation, Data curation, Validation, Writing - review & editing. **Milena Fini:** Resources, Supervision. **Adriana Bigi:** Conceptualization, Methodology, Supervision, Resources, Writing - original draft, Writing - review & editing. **Daria Giacomini:** Conceptualization, Methodology, Supervision, Resources, Visualization, Writing - review & editing.

Acknowledgements

The paper is published with the contribution of the Department of Excellence program financed by the Ministry of Education, University and Research (MIUR, L. 232 del 01/12/2016). Authors are also grateful to IRCCS Istituto Ortopedico Rizzoli (funds Ministero della Salute – Ricerca Corrente, and 5x1000/2017, code 730164),to the Italian Ministry of Education, University and Research (D.G.) (PRIN 2015 project 20157WW5EH) and to the University of Bologna. D.G. would like to thank Ms. Maria Edith Casacchia for technical assistance.

Appendix A. Supplementary data

Supplementary material related to this article can be found, in the online version, at doi:https://doi.org/10.1016/j.colsurfb.2021.111580.

References

[1] A. Bigi, E. Boanini, Functionalized biomimetic calcium phosphates for bone tissue repair, J. Appl. Biomater. Funct. Mater. 15 (2017) e313–e325, https://doi.org/10.5301/jabfm.5000367.
[2] S.V. Dorozhkin, Functionalized calcium orthophosphates ($CaPO_4$) and their biomedical applications, J. Mater. Chem. B 7 (2019) 7471–7489, https://doi.org/10.1039/c9tb01976f.
[3] V. Uskoković, Ion-doped hydroxyapatite: an impasse or the road to follow? Ceram. Int. (2020) https://doi.org/10.1016/j.ceramint.2020.02.001.
[4] P.J. Marie, Strontium ranelate: a novel mode of action optimizing bone formation and resorption, Osteoporos. Int. 16 (2005) S7–S10, https://doi.org/10.1007/s00198-004-1753-8.
[5] V. Uskoković, I. Janković-Častvan, V.M. Wu, Bone mineral crystallinity governs the orchestration of ossification and resorption during bone remodeling, ACS Biomater. Sci. Eng. 5 (2019) 3483–3498, https://doi.org/10.1021/acsbiomaterials.9b00255.
[6] N. Neves, D. Linhares, G. Costa, C.C. Ribeiro, M.A. Barbosa, In vivo and clinical application of strontium-enriched biomaterials for bone regeneration: a systematic review, Bone Joint Res. 6 (2017) 366–375, https://doi.org/10.1302/2046-3758.66.BJR-2016-0311.R1.
[7] C. Capuccini, P. Torricelli, E. Boanini, M. Gazzano, R. Giardino, A. Bigi, Interaction of Sr-doped hydroxyapatite nanocrystals with osteoclast and osteoblast-like cells, J. Biomed. Mater. Res. Part A 89 (2009) 594–600, https://doi.org/10.1002/jbm.a.31975.
[8] E. Boanini, P. Torricelli, M. Fini, A. Bigi, Osteopenic bone cell response to strontium- substituted hydroxyapatite, J. Mater. Sci. Mater. Med. 22 (2011) 2079–2088, https://doi.org/10.1007/s10856-011-4379-3.
[9] Y.F. Li, X.P. Shui, L. Zhang, J. Hu, Cancellous bone healing around strontium-doped hydroxyapatite in osteoporotic rats previously treated with zoledronic acid, J. Biomed. Mater. Res. B Appl. Biomater. 104 (2016) 476–481, https://doi.org/10.1002/jbm.b.33417.
[10] F. Salamanna, G. Giavaresi, A. Parrilli, P. Torricelli, E. Boanini, A. Bigi, M. Fini, Antiresorptive properties of strontium substituted and alendronate functionalized hydroxyapatite nanocrystals in an ovariectomized rat spinal arthrodesis model, Mater. Sci. Eng. C 95 (2019) 355–362, https://doi.org/10.1016/j.msec.2017.11.016.
[11] E. Boanini, P. Torricelli, F. Sima, E. Axente, M. Fini, I.N. Mihailescu, A. Bigi, Gradient coatings of strontium hydroxyapatite/zinc β-tricalcium phosphate as a tool to modulate osteoblast/osteoclast response, J. Inorg. Biochem. 183 (2018) 1–8, https://doi.org/10.1016/j.jinorgbio.2018.02.024.
[12] S. Bagherifard, Mediating bone regeneration by means of drug eluting implants: from passive to smart strategies, Mater. Sci. Eng. C 71 (2017) 1241–1252, https://doi.org/10.1016/j.msec.2016.11.011.

[13] E. Boanini, P. Torricelli, M. Gazzano, E. Della Bella, M. Fini, A. Bigi, Combined effect of strontium and zoledronate on hydroxyapatite structure and bone cell responses, Biomaterials 35 (2014) 5619–5626, https://doi.org/10.1016/j.biomaterials.2014.03.053.

[14] Q. Wei, T.L.M. Pohl, A. Seckinger, J.P. Spatz, E.A. Cavalcanti-Adam, Regulation of integrin and growth factor signaling in biomaterials for osteodifferentiation, Beilstein J. Org. Chem. 11 (2015) 773–783, https://doi.org/10.3762/bjoc.11.87.

[15] R.O. Hynes, Integrins: bidirectional, allosteric signaling machines, Cell 110 (2002) 673–687, https://doi.org/10.1016/s0092-8674(02)00971-6.

[16] M. Barczyk, S. Carracedo, D. Gullberg, Integrins, Cell Tissue Res. 339 (2010) 269–280, https://doi.org/10.1007/s00441-009-0834-6.

[17] a) P.J. Marie, Targeting integrins to promote bone formation and repair, Nat. Rev. Endocrinol. 9 (2013) 288–295, https://doi.org/10.1038/nrendo.2013.4;
b) I.P. Geoghegan, D.A. Hoey, L.M. Mc Namara, Integrins in osteocyte biology and mechanotransduction, Curr. Osteoporos. Rep. 17 (2019) 195–206, https://doi.org/10.1007/s11914-019-00520-00522.

[18] L.T. Duong, P. Lakkakorpi, I. Nakamura, G.A. Rodan, Integrins and signaling in osteoclast function, Matrix Biol. 19 (2000) 97–105, https://doi.org/10.1016/s0945-053x(00)00051-2.

[19] a) C.H. Damsky, Extracellular matrix-integrin interactions in osteoblast function and tissue remodelling, Bone 25 (1999) 95–96, https://doi.org/10.1016/s8756-3282(99)00106-4;
b) M. Brunner, N. Mandier, T. Gautier, G. Chevalier, A.S. Ribba, P. Guardiola, M. R. Block, D. Bouvard, β1 integrins mediate the BMP2 dependent transcriptional control of osteoblast differentiation and osteogenesis, PLoS One 13 (2018), e0196021, https://doi.org/10.1371/journal.pone.0196021.

[20] a) R.K. Globus, D. Amblard, Y. Nishimura, U.T. Iwaniec, J.-B. Kim, E.A. C. Almeida, C.D. Damsky, T.J. Wronski, M.C.H. van der Meulen, Skeletal phenotype of growing transgenic mice that express a function-perturbing form of β_1 integrin in osteoblasts, Calcif. Tissue Int. 76 (2005) 39–49, https://doi.org/10.1007/s00223-004-0309-4;
b) H.B. Lopes, G.P. Freitas, C.N. Elias, C. Tye, J.L. Stein, G.S. Stein, J.B. Lian, A. L. Rosa, M.M. Beloti, Participation of integrin β_3 in osteoblast differentiation induced by titanium with nano or microtopography, J. Biomed. Mater. Res. Part A 107A (2019) 1303–1313, https://doi.org/10.1002/jbm.a.36643;
c) U.T. Iwaniec, T.J. Wronski, D. Amblard, Y. Nishimura, M.C.H. van der Meulen, C.E. Wade, M.A. Bourgeois, C.D. Damsky, R.K. Globus, Effects of disrupted β_1-integrin function on the skeletal response to short-term hindlimb unloading in mice, J. Appl. Physiol. 98 (2005) 690–696, https://doi.org/10.1152/japplphysiol.00689.2004.

[21] C.R. Yeh, J.J. Chiu, C.I. Lee, P.L. Lee, Y.T. Shih, J.S. Sun, S. Chien, C.K. Cheng, Estrogen augments shear stress-induced signaling and gene expression in osteoblast-like cells via estrogen receptor-mediated expression of β1-integrin, J. Bone Miner. Res. 25 (2010) 627–639, https://doi.org/10.1359/jbmr.091008.

[22] S.J. Park, J. Gadi, K.W. Cho, K.J. Kim, S.H. Kim, H.S. Jung, S.K. Lim, The forkhead transcription factor Foxc2 promotes osteoblastogenesis via up-regulation of integrin β1 expression, Bone 49 (2011) 428–438, https://doi.org/10.1016/j.bone.2011.05.012.

[23] R. Dimitriou, E. Jones, D. McGonagle, P.V. Giannoudis, Bone regeneration: current concepts and future directions, BMC Med. 9 (2011) 66, https://doi.org/10.1186/1741-7015-9-66.

[24] R.M. Samsonraj, M. Raghunath, V. Nurcombe, J.H. Hui, A.J. van Wijnen, S. M. Cool, Concise review: multifaceted characterization of human mesenchymal stem cells for use in regenerative medicine, Stem Cells Transl. Med. 6 (2017) 2173–2185, https://doi.org/10.1002/sctm.17-0129.

[25] J.E. Frith, R.J. Mills, J.E. Hudson, J.J. Cooper-White, Tailored integrin extracellular matrix interactions to direct human mesenchymal stem cell differentiation, Stem Cells Dev. 21 (2012) 2442–2456, https://doi.org/10.1089/scd.2011.0615.

[26] S. Gronthos, P.J. Simmons, S.E. Graves, P.G. Robey, Integrin-mediated interactions between human bone marrow stromal precursor cells and the extracellular matrix, Bone 28 (2001) 174–181, https://doi.org/10.1016/s8756-3282(00)00424-5.

[27] Z. Hamidouche, O. Fromigué, J. Ringe, T. Häupl, P. Vaudin, J.-C. Pagès, S. Srouji, E. Livne, P.J. Marie, Priming integrin α_5 promotes human mesenchymal stromal cell osteoblast differentiation and osteogenesis, Proc. Natl. Acad. Sci. U. S. A. 106 (2009) 18587–18591, https://doi.org/10.1073/pnas.0812334106.

[28] S. Mukherjee, N. Raje, J.A. Schoonmaker, J.C. Liu, T. Hideshima, M.N. Wein, D. C. Jones, S. Vallet, M.L. Bouxsein, S. Pozzi, S. Chhetri, Y.D. Seo, J.P. Aronson, C. Patel, M. Fulciniti, L.E. Purton, L.H. Glimcher, J.B. Lian, G. Stein, K.C. Anderson, D.T. Scadden, Pharmacologic targeting of a stem/progenitor population in vivo is associated with enhanced bone regeneration in mice, J. Clin. Invest. 118 (2008) 491–504, https://doi.org/10.1172/JCI33102.

[29] N. Huettner, T.R. Dargaville, A. Forget, Discovering cell-adhesion peptides in tissue engineering: beyond RGD, Trends Biotechnol. 36 (2018) 372–383, https://doi.org/10.1016/j.tibtech.2018.01.008.

[30] D. Puleo, R. Bizios, RGDS tetrapeptide binds to osteoblasts and inhibits fibronectin-mediated adhesion, Bone 12 (1991) 271–276, https://doi.org/10.1016/8756-3282(91)90075-T.

[31] A. Mardilovich, E. Kokkoli, Biomimetic peptide-amphiphiles for functional biomaterials: the role of GRGDSP and PHSRN, Biomacromolecules 5 (2004) 950–957, https://doi.org/10.1021/bm0344351.

[32] K.M. Hennessy, W.C. Clem, M.C. Phipps, A.A. Sawyer, F.M. Shaikh, S.L. Bellis, The effect of RGD peptides on osseointegration of hydroxyapatite biomaterials, Biomaterials 29 (2008) 3075–3083, https://doi.org/10.1016/j.biomaterials.2008.04.014.

[33] S.L. Bellis, Advantages of RGD peptides for directing cell association with biomaterials, Biomaterials 32 (2011) 4205–4210, https://doi.org/10.1016/j.biomaterials.2011.02.029.

[34] a) P. Galletti, R. Soldati, M. Pori, M. Durso, A. Tolomelli, L. Gentilucci, S. D. Dattoli, M. Baiula, S. Spampinato, D. Giacomini, Targeting integrins $\alpha_v\beta_3$ and $\alpha_5\beta_1$ with new β-lactam derivatives, Eur. J. Med. Chem. 83 (2014) 284–293, https://doi.org/10.1016/j.ejmech.2014.06.041;
b) M. Baiula, P. Galletti, G. Martelli, R. Soldati, L. Belvisi, M. Civera, S.D. Dattoli, S.M. Spampinato, D. Giacomini, New β-lactam derivatives modulate cell adhesion and signaling mediated by RGD-binding and leukocyte integrins, J. Med. Chem. 59 (2016) 9721–9742, https://doi.org/10.1021/acs.jmedchem.6b00576;
c) G. Martelli, M. Baiula, A. Caligiana, P. Galletti, L. Gentilucci, R. Artali, S. Spampinato, D. Giacomini, Could dissecting the molecular framework of β-lactam integrin ligands enhance selectivity? J. Med. Chem. 62 (2019) 10156–10166, https://doi.org/10.1021/acs.jmedchem.9b01000.

[35] G. Martelli, N. Bloise, A. Merlettini, G. Bruni, L. Visai, M.L. Focarete, D. Giacomini, Combining biologically active β-lactams integrin agonists with poly(l-lactic acid) nanofibers: enhancement of human mesenchymal stem cell adhesion, Biomacromolecules 21 (2020) 1157–1170, https://doi.org/10.1021/acs.biomac.9b01550.

[36] D. Giacomini, P. Torricelli, G.A. Gentilomi, E. Boanini, M. Gazzano, F. Bonvicini, E. Benetti, R. Soldati, G. Martelli, K. Rubini, A. Bigi, Monocyclic β-lactams loaded on hydroxyapatite: new biomaterials with enhanced antibacterial activity against resistant strains, Sci. Rep. 7 (2017) 2712, https://doi.org/10.1038/s41598-017-02943-2.

[37] L.R. Snyder, Classification of the solvent properties of common liquids, J. Chromatogr. 92 (1974) 223–230, https://doi.org/10.1016/S0021-9673(00)85732-5.

[38] B.N. Bhadra, K.H. Cho, N.A. Khan, D.Y. Hong, S.H. Jhung, Liquid-phase adsorption of aromatics over a metal-organic framework and activated carbon: effects of hydrophobicity/ hydrophilicity of adsorbents and solvent polarity, J. Phys. Chem. C 119 (2015) 26620–26627, https://doi.org/10.1021/acs.jpcc.5b09298.

[39] G.B. Deacon, R.J. Phillips, Relationships between the carbon-oxygen stretching frequencies of carboxylato complexes and the type of carboxylate coordination, Coord. Chem. Rev. 33 (1980) 227–250, https://doi.org/10.1016/S0010-8545(00)80455-5.

[40] G. Tarone, E. Hirsch, M. Brancaccio, M. De Acetis, L. Barberis, F. Balzac, S.F. Retta, C. Botta, F. Altruda, L. Silengo, Integrin function and regulation in development, Int. J. Dev. Biol. 44 (2000) 725–731. PMID: 11061437.

[41] S.M. Frisch, E. Ruoslahti, Integrins and anoikis, Curr. Opin. Cell Biol. 9 (1997) 701–706, https://doi.org/10.1016/s0955-0674(97)80124-x.

[42] A. Di Benedetto, G. Brunetti, F. Posa, A. Ballini, F.R. Grassi, G. Colaianni, S. Colucci, E. Rossi, E.A. Cavalcanti-Adam, L. Lo Muzio, M. Grano, G. Mori, Osteogenic differentiation of mesenchymal stem cells from dental bud: role of integrins and cadherins, Stem Cell Res. 15 (2015) 618–628, https://doi.org/10.1016/j.scr.2015.09.011.

[43] Q. Chen, P. Shou, L. Zhang, C. Xu, C. Zheng, Y. Han, W. Li, Y. Huang, X. Zhang, C. Shao, A.I. Roberts, A.B. Rabson, G. Ren, Y. Zhang, Y. Wang, D.T. Denhardt, Y. Shi, An osteopontin-integrin interaction plays a critical role in directing adipogenesis and osteogenesis by mesenchymal stem cells, Stem Cells 32 (2014) 327–337, https://doi.org/10.1002/stem.1567.

[44] M. Fonovic, B. Turk, Cysteine cathepsins and extracellular matrix degradation, Biochim. Biophys. Acta 1840 (2014) 2560–2570, https://doi.org/10.1016/j.bbagen.2014.03.017.

[45] X. Ren, W.H. Shan, L.L. Wei, C.C. Gong, D.S. Pei, ACP5: its structure, distribution, regulation and novel functions, Anticancer Agents Med. Chem. 18 (2018) 1082–1090, https://doi.org/10.2174/1871520618666180411123447.

[46] N.A. Diepenhorst, K. Leach, A.N. Keller, P. Rueda, A.E. Cook, T.L. Pierce, C. Nowell, P. Pastoureau, M. Sabatini, R.J. Summers, W.N. Charman, P.M. Sexton, A. Christopoulos, C.J. Langmead, Divergent effects of strontium and calcium-sensing receptor positive allosteric modulators (calcimimetics) on human osteoclast activity, Br. J. Pharmacol. 175 (2018) 4095–4108, https://doi.org/10.1111/bph.14344.

[47] W. Querido, A.L. Rossi, M. Farina, The effects of strontium on bone mineral: a review on current knowledge and microanalytical approaches, Micron 80 (2016) 122–134, https://doi.org/10.1016/j.micron.2015.10.006.

[48] M.N. Kozhevnikova, A.S. Mikaelyan, V.I. Starostin, Molecular and genetic regulation of osteogenic differentiation of mesenchymal stromal cells, Biol. Bull. Russ. Acad. Sci. 35 (2008) 223–232, https://doi.org/10.1134/S1062359008030011.

[49] C.J. Chung, H.Y. Long, Systematic strontium substitution in hydroxyapatite coatings on titanium via micro-arc treatment and their osteoblast/osteoclast responses, Acta Biomater. 7 (2011) 4081–4087, https://doi.org/10.1016/j.actbio.2011.07.004.